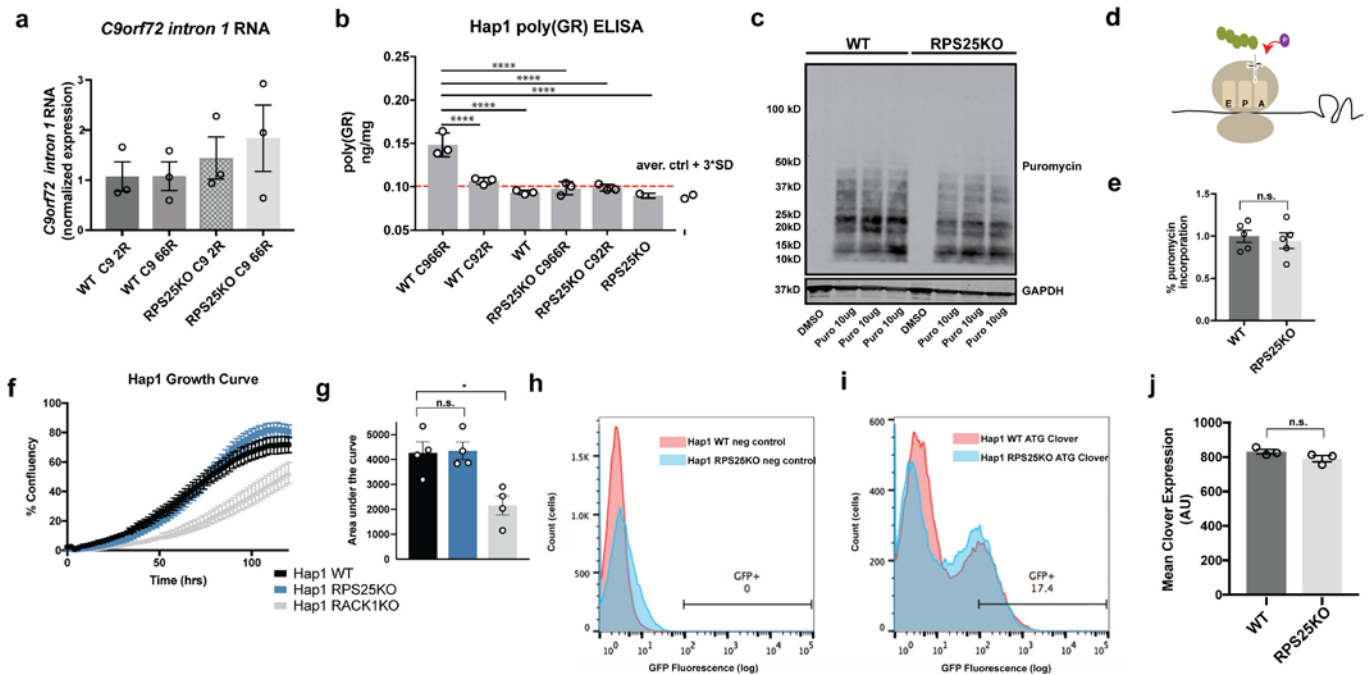


Supplementary Figure 1

Figure S1: Deletion of RPS25A does not affect C9 RNA nor does it affect ATG GFP expression.

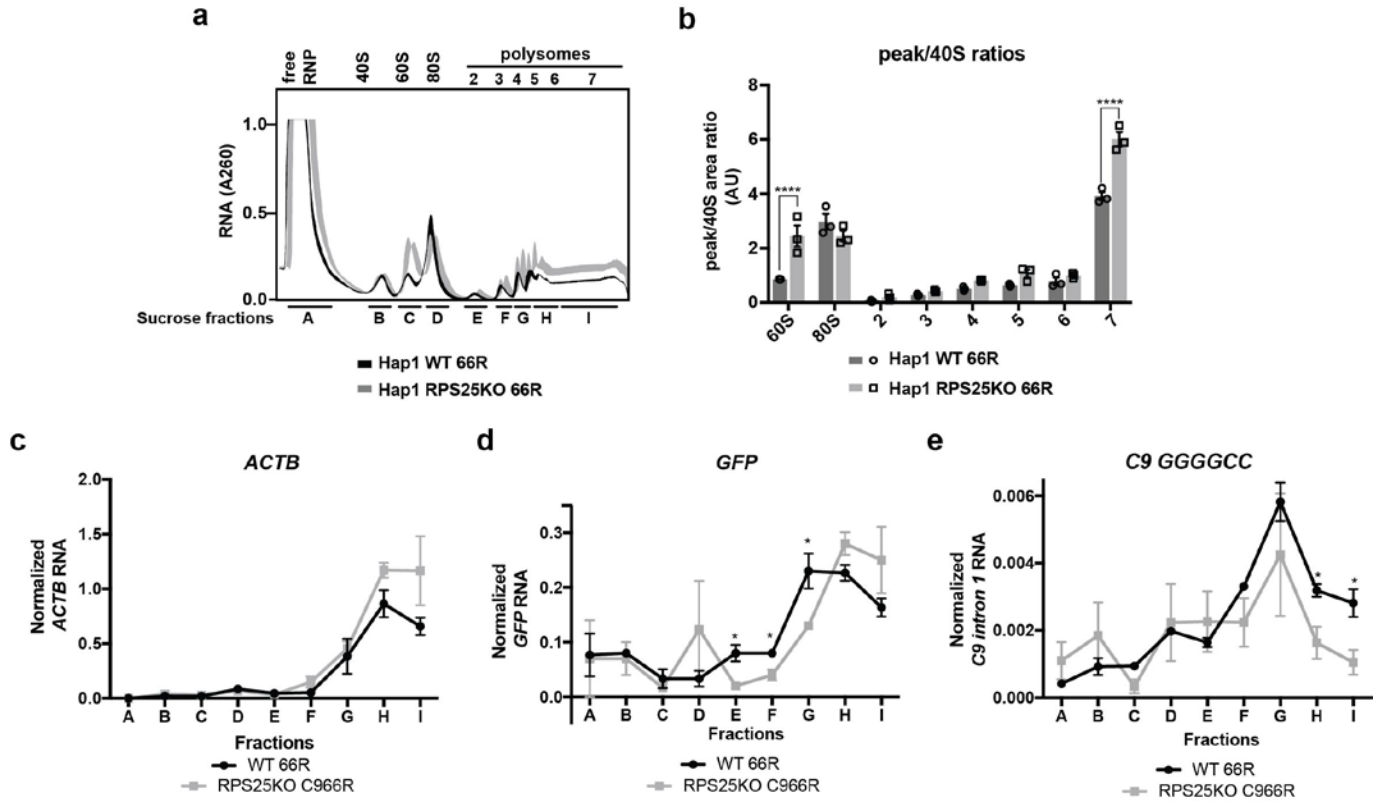
(a) Details of C9 2R and 66R constructs in yeast galactose-inducible vector (GAL1) and in mammalian expression vector driven by a CAG promoter. Each potential reading frame is tagged in with a different epitope as indicated. For human cell culture experiments, the poly(GA) frame is detected using the HA epitope tag. (b) 113bp of endogenous *C9orf72* sequence 5' of the repeats is included in the construct and sequence details are provided. (c) 99bp of endogenous *C9orf72* sequence 3' of the repeats are included and sequence details are provided. (d) RT-qPCR analysis of *C9orf72* intron 1 normalized to yeast *ACT1* from wildtype and *rps25A*Δ yeast expressing empty vector, C9 2R and C9 66R (two-tailed, unpaired t-test; n = 3 independent yeast transformants; n.s., not significant, p=0.1587; mean +/- s.e.m.). (e) Immunoblot of wildtype and *rps25A*Δ yeast expressing ATG-GFP. (f) Quantification of (e). For this and all subsequent supplemental figures, full statistics can be found in **Table S4** and uncropped immunoblots can be found in **Fig. S11**.



Supplementary Figure 2

Figure S2: Knock out of RPS25 in Hap1 cells does not reduce C9 RNA levels nor does it affect translation globally.

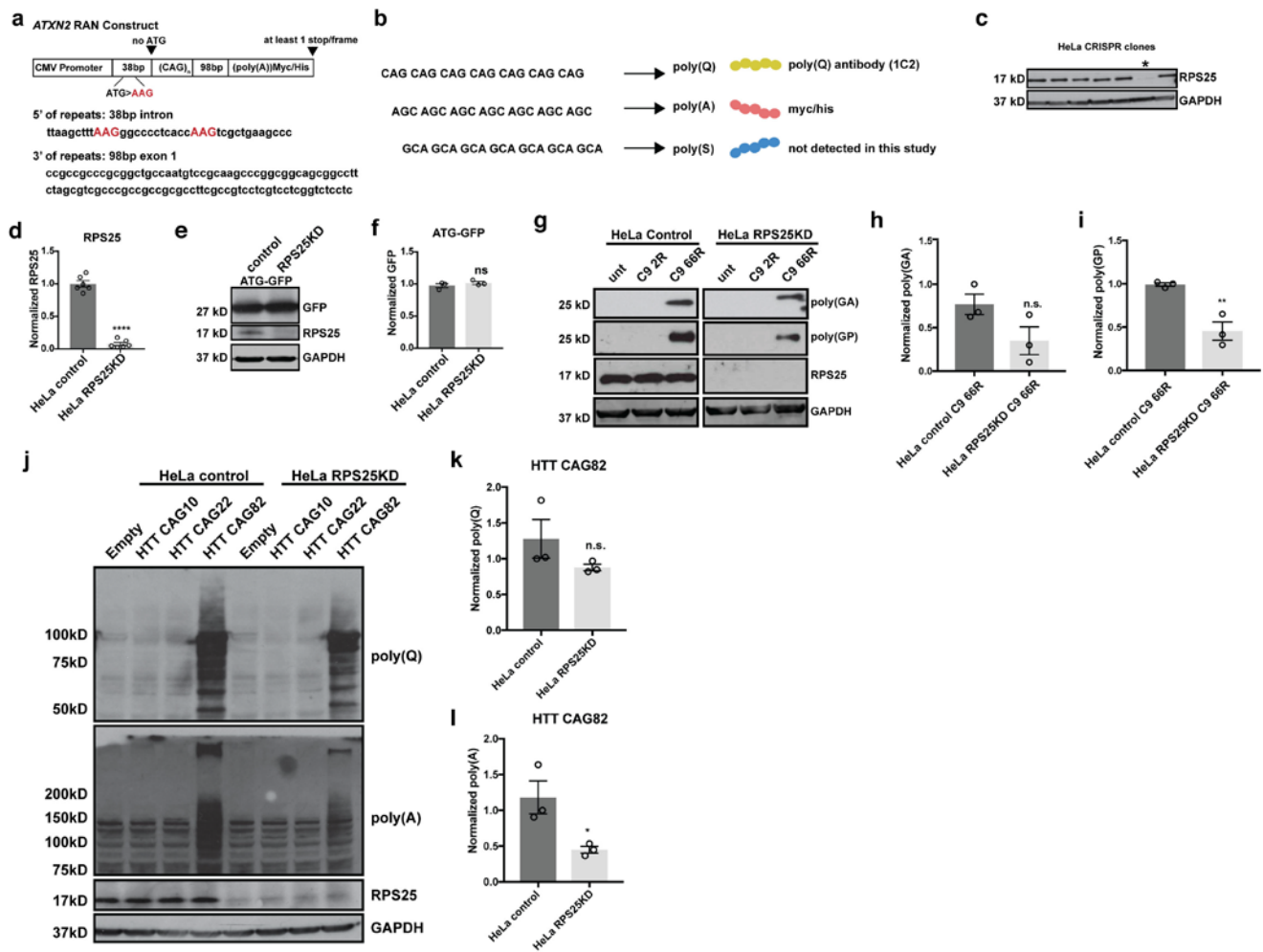
(a) C9 RNA levels normalized to *ActB* RNA in Hap1 wildtype versus RPS25 knockout cells as measured by RT-qPCR (two-tailed, unpaired t-test; $n=3$ independent cell culture experiments; wildtype C9 66R versus RPS25KO C9 66R, ns, not significant, $p=0.3530$; mean \pm s.e.m.). (b) Full poly(GR) assay in **Fig. 1h** shown. Immunoassay illustrates RPS25 KO in Hap1 cells reduces poly(GR) levels to that of Hap1 WT transfected with empty vector (ordinary one-way ANOVA with Tukey's multiple comparisons, $n = 3$ independent cell culture experiments; **** $p < 0.0001$; mean \pm s.e.m.). (c) Immunoblot of puromycin incorporation assay for wildtype and RPS25KO cells. Puromycin incorporation assay to assess levels of nascent translation. Puromycin is incorporated at similar levels in wildtype and RPS25 KO. (d) Schematic for puromycin incorporation assay. (e) Quantification of puromycin blot in (c) (two-tailed, unpaired t-test; $n=3$; n.s., not significant, $p=0.6653$; mean \pm s.e.m.). (f) Growth curve analysis comparing Hap1 wildtype and RPS25 KO. Hap1 RACK1KO cells are provided for comparison of another non-essential ribosomal protein deletion. (g) Area under the growth curves are quantified. Growth curve analysis indicates that Hap1 wildtype and RPS25 KO cells grow similarly under normal culture conditions (two-tailed, unpaired t-test; $n=3$ independent cell culture experiments; * $p=0.0108$, ns, not significant $p=0.9001$; mean \pm s.e.m.). (h) Flow cytometry analysis of untransfected Hap1 wildtype and RPS25KO cells. Cells are analyzed for GFP (FITC) expression and used to determine cut off for GFP positive cell population. (i) Analysis of ATG Clover expression in transfected Hap1 wildtype and RPS25 knockout cells. Cell fluorescence distribution illustrates similar population expression. (j) Mean Clover expression of GFP positive (GFP+) populations as indicated in (h) and (i) are quantified (two-tailed, unpaired t-test; $n=3$ independent cell culture experiments; n.s., not significant $p=0.1469$; mean \pm s.e.m.).



Supplementary Figure 3

C9 RNA is specifically depleted in heavy polysome fractions of RPS25KO cells.

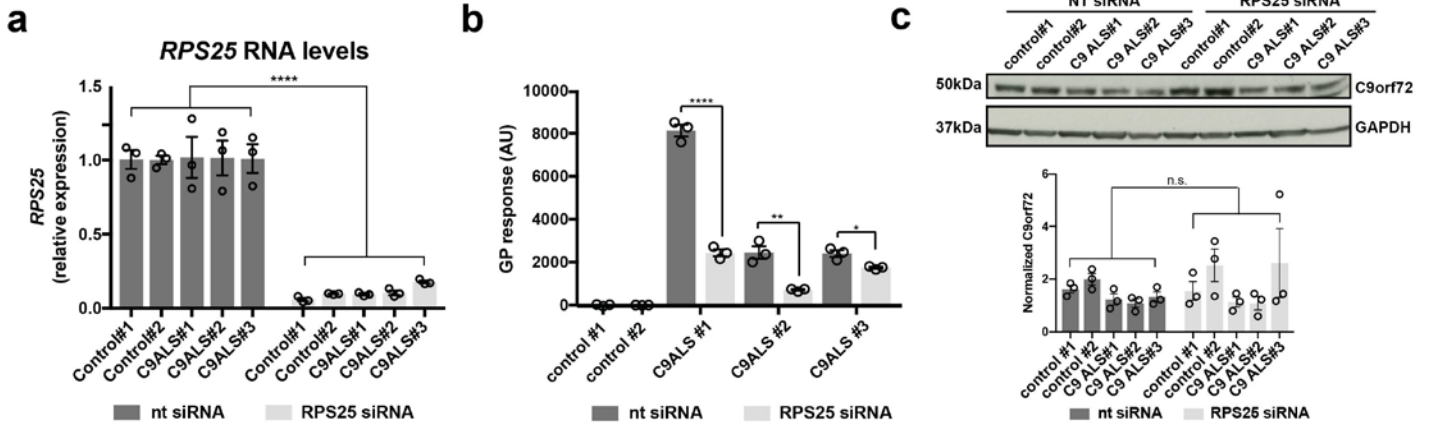
(a) Polysome profiling to compare global translation between wildtype and RPS25KO cells. A260 profiles from sucrose gradient fractions separating RNA by number of bound polysomes (n=3 independent cell culture experiments; error bars reflected in line thickness, s.e.m.). (b) Area under each peak is quantified and normalized to the 40S peak. Peak-to-40S ratios are compared between wildtype and RPS25KO cells. 60S/40S and area under heavy polysome region 7/40S are significantly higher in RPS25KO cells (two-tailed, unpaired t-test; n=3 independent cell culture experiments; ****p<0.0001; mean +/- s.e.m.). (c-f) For non-significant results, please see **Table S4** for p-values. (c) RT-qPCR of *ACTB* RNA from fractions detailed in (a). *ACTB* RNA is not significantly changed in polysome fractions (two-tailed, unpaired t-test of wildtype versus RPS25KO cells; n=3 cell culture experiments for all but wildtype fraction c which has n=2; mean +/- s.e.m.). (d) RT-qPCR of *GFP* RNA expressed from a GFP plasmid co-transfected with C9 66R. *GFP* RNA levels in lighter polysome fractions (E, F, and G) are lower in RPS25KO cells. *GFP* RNA levels in heavy polysomes (H and I) are not statistically different (two-tailed, unpaired t-test; n=3 cell culture experiments for all but wildtype fraction c which has n=2; (E) *=0.0171, (F) *p=0.0257, (G) *p=0.0376; mean +/- s.e.m.). (e) RT-qPCR of *C9 intron 1* RNA levels from fractions detailed in (a). There is a significant decrease in *C9 intron 1* RNA from heavy polysomes in RPS25KO cells (two-tailed, unpaired t-test; n=3 cell culture experiments for all but wildtype fraction c which has n=2; (H) *p=0.0388, (I) *p=0.0336; mean +/- s.e.m.).



Supplementary Figure 4

Figure S4: RPS25 reduction in HeLa cells lowers GGGGCC and CAG RAN translation products.

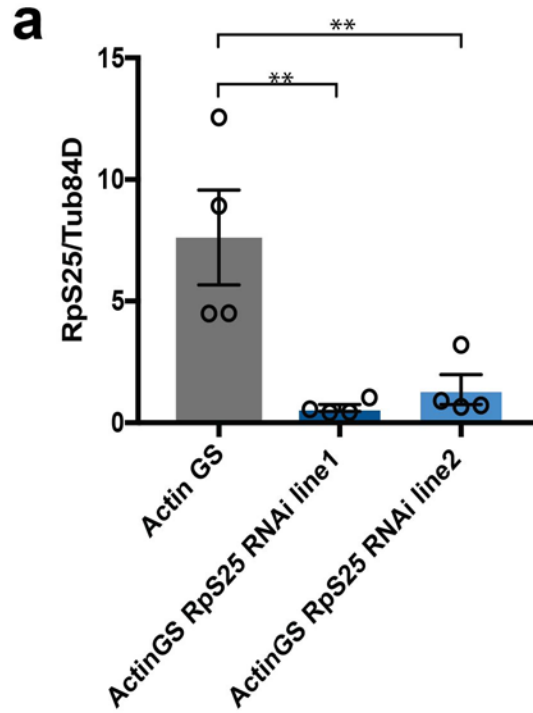
(a) Schematic of the *ATXN2* RAN construct is provided. All ATGs upstream of the CAG repeats are mutated to AAG and myc/his epitope tag is placed C-terminally in the poly(A) frame. (b) Potential sense CAG reading frames and RAN translation products are indicated. Antibodies used to detect the poly(A) and poly(Q) products in this study are detailed. (c) Immunoblot identifying a CRISPR-derived HeLa clone with reduced RPS25 expression (indicated by *). (d) Quantification of RPS25 normalized to GAPDH of immunoblot in Fig. 1i. RPS25 expression is reduced to ~10% of wildtype HeLa cells. Control HeLa cells are derived from the same HeLa-Cas9 BFP population infected with a non-targeting guide (two-tailed, unpaired t-test; $n=6$ cell culture experiments; **** $p<0.0001$, mean \pm s.e.m.). (e) Immunoblot of lysates from HeLa cells transfected with ATG-GFP. (f) Quantification of (e) illustrates no difference in ATG-initiated GFP expression in control versus RPS25KD mutant cells (two-tailed, unpaired t-test; $n=3$ independent cell culture experiments; n.s., not significant $p=0.3616$; mean \pm s.e.m.). (g) Immunoblot of HeLa lysates transfected with C9 2R or C9 66R plasmids. (h) Quantification of poly(GA) from (g) indicates there is a trend, but not significant, decrease in RPS25KD cells (two-tailed, unpaired t-test; $n=3$ cell culture experiments; n.s., not significant $p=0.1020$; mean \pm s.e.m.). (i) Quantification of poly(GP) from (g) indicates a significant decrease in RPS25KD cells (two-tailed unpaired t-test; $n=3$ cell culture experiments; ** $p=0.0072$; mean \pm s.e.m.). (j) Immunoblots of lysates from HeLa cells transfected with variable *HTT* CAG repeats. *HTT* CAG RAN poly(A) products are only detected in CAG82 repeats. (k) Quantification of poly(Q) from (j). Poly(Q) initiates from the native ATG of *HTT* and is not RAN translated. Poly(Q) is not significantly decreased in RPS25KD cells (two-tailed, unpaired t-test; $n=3$ cell culture experiments; n.s., not significant $p=0.2154$; mean \pm s.e.m.). (l) Quantification of poly(A) from (j). Antibody detects C-terminal epitope in the RAN translated poly(A) frame. Poly(A) products are decreased in RPS25KD cells (two-tailed, unpaired, t-test; $n=3$ independent cell culture experiments; * $p=0.0358$; mean \pm s.e.m.).



Supplementary Figure 5

Figure S5: siRNA reduction of RPS25 in iPSCs.

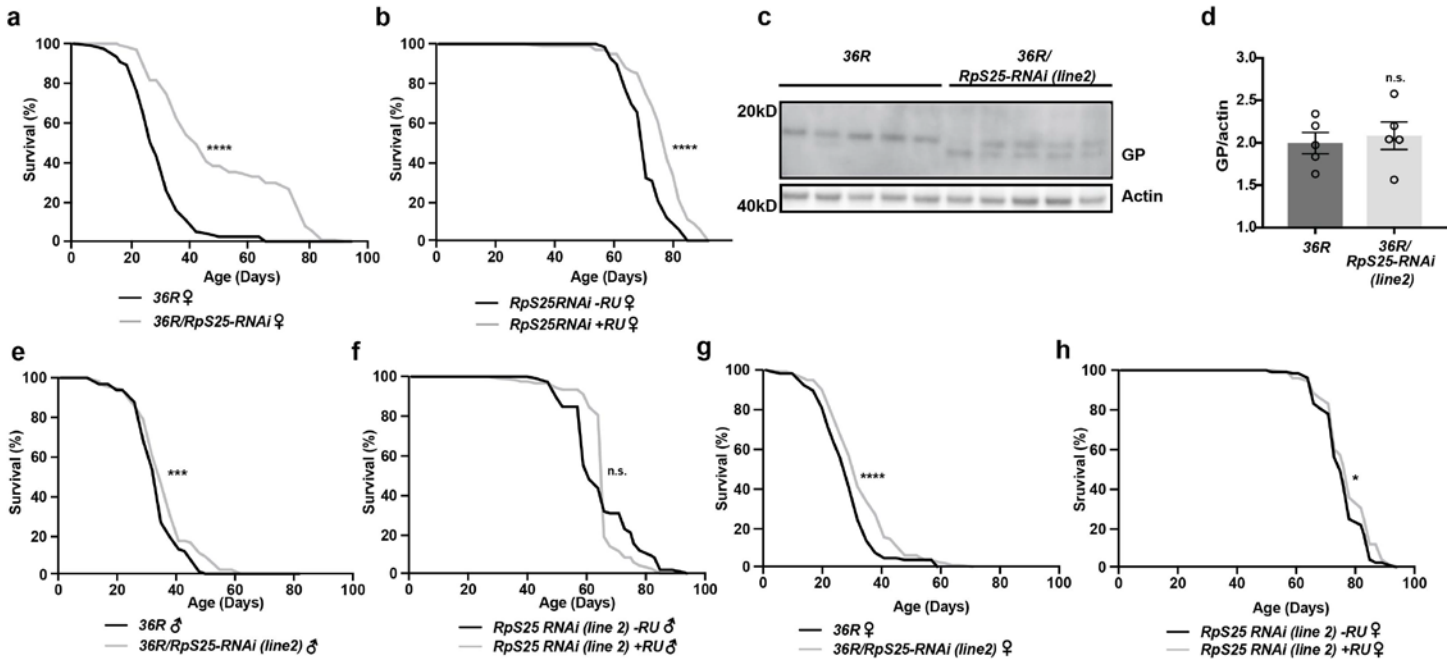
(a) RT-qPCR of *RPS25* RNA normalized to *ActB* RNA from control and c9ALS patient-derived iPSCs treated with non-targeting or RPS25-targeting siRNA indicating a significant reduction in *RPS25* RNA in cells treated with RPS25-targeting siRNA (One-way ANOVA; n=3 cell culture experiments per line per treatment; ****p<0.0001; mean +/- s.e.m.). (b) Unnormalized poly(GP) immunoassay data presented in Fig. 2b (two-tailed, unpaired t-test; n=3 cell culture experiments; *p=0.0161, **p=0.0039, ****p<0.0001; mean +/- s.e.m.). (c) Immunoblot and quantification for C9orf72 protein (long isoform) in control and c9ALS patient-derived iPSCs treated with non-targeting or RPS25-targeting siRNA. There was no significant change in comparing non-targeted and RPS25-targeted groups (Two-way ANOVA with Sidak's multiple comparison test; n=3 cell culture experiments; n.s., not significant p=0.3131; not shown on graph is non-targeting versus RPS25-targeting siRNA treatment for each iPSC line was also not significant; mean +/- s.e.m.).



Supplementary Figure 6

Figure S6: RPS25-RNAi induction in *Drosophila* reduces *RPS25* RNA.

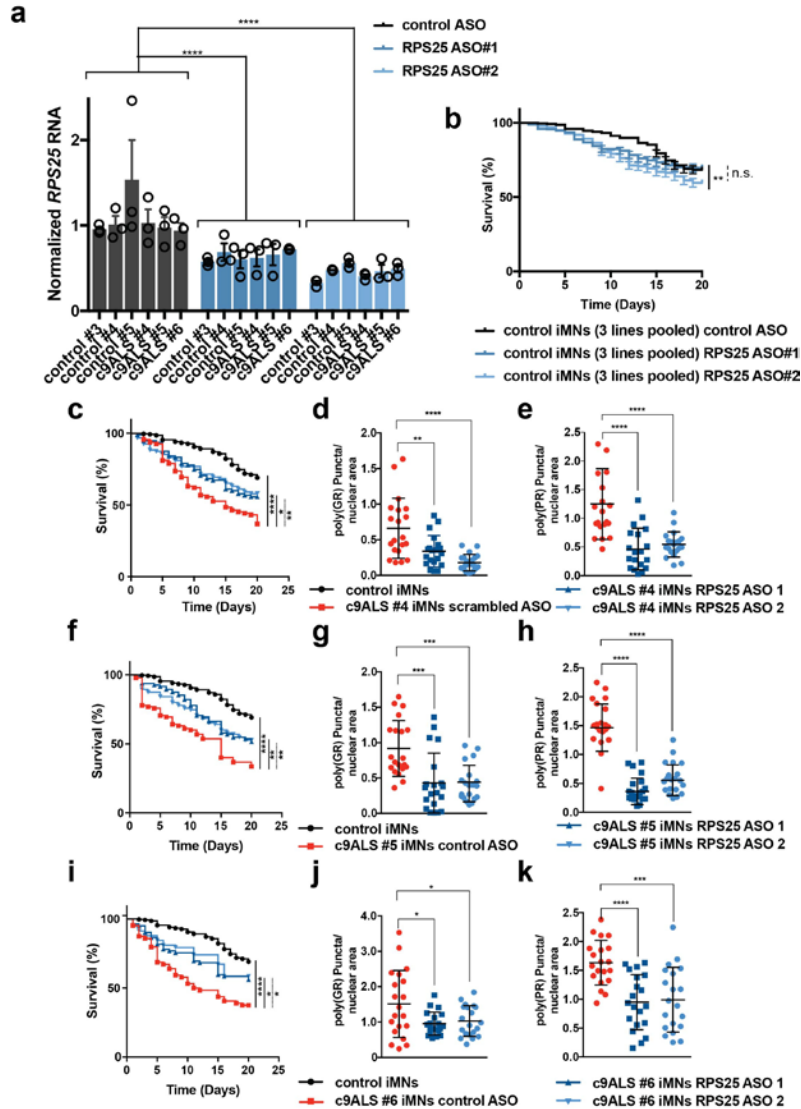
(a) RT-qPCR of *RPS25* RNA normalized to *Tub84D* from *Drosophila* expressing RPS25-RNAi (One-way ANOVA with Dunnett's multiple comparison test; n=4 replicates of 8 individual pooled flies; (RpS25 RNAi line1) p=0.0044, (RpS25 RNAi line2) p=0.0086; mean +/- s.e.m.) Genotypes: *actinGS*, *actinGS*, *Rps25 line1*, *actinGS*, *Rps25 line2*.



Supplementary Figure 7

Figure S7: Rps25 RNAi extends lifespan in a 36R *Drosophila* model.

(a) Survival curves of female flies expressing 36(GGGGCC) alone (36R) or together with Rps25 RNAi in adult neurons, showing a lifespan increase in the presence of Rps25 RNAi (**** $p < 0.0001$ by chi-squared log-rank test, $n > 100$ flies per genotype). Genotypes: *UAS-36(GGGGCC)/+; elavGS* ($n = 121$ flies), *UAS-36(GGGGCC)/UAS-RpS25RNAi{KK107958}; elavGS/+* ($n = 130$ flies). **(b)** Expression of Rps25 RNAi alone in adult neurons (+RU) modestly extended lifespan of female flies relative to the un-induced control (-RU) (**** $p < 0.0001$ by chi-squared log-rank test, $n = 70$ uninduced and $n = 101$ RNAi induced flies). Genotype: *UAS-RpS25RNAi{KK107958}/+; elavGS/+*. **(c)** Immunoblot of fly heads expressing 36(GGGGCC) alone (control) or together with Rps25 RNAi line 2 in adult neurons, showing a modest reduction of poly(GP) levels in RPS25 RNAi induced flies. Genotypes: *UAS-36(GGGGCC)/+; elavGS*, *UAS-36(GGGGCC)/+; RpS25RNAi{GD10582}/elavGS*. **(d)** Quantification of (c) (unpaired, two-tailed t-test; $n = 5$ biological replicates; ns, not significant $p = 0.6847$, mean \pm s.e.m.). **(e)** Survival curves of male flies expressing 36R alone or together with a second Rps25 RNAi line in adult neurons, showing a lifespan increase in the presence of Rps25RNAi (** $p = 0.0056$ by chi-squared log-rank test, $n > 97$ flies per genotype). Genotypes: *UAS-36(GGGGCC)/+; elavGS* ($n = 97$ flies), *UAS-36(GGGGCC); RpS25RNAi{GD10582}/elavGS/+* ($n = 113$ flies). **(f)** Expression of Rps25 RNAi line 2 alone in adult neurons (+RU) did not affect survival of male flies relative to the un-induced control (-RU) (chi-squared log-rank test; $n = 112$ uninduced and $n = 123$ RNAi induced flies); n.s., not significant $p = 0.6123$). Genotypes: *UAS-RpS25RNAi{GD10582}/elavGS*. **(g)** Survival curves of female flies expressing 36(GGGGCC) alone (36R) or together with Rps25 RNAi line 2 in adult neurons, showing a lifespan increase in the presence of Rps25 RNAi (**** $p < 0.0001$ by chi-squared log-rank test; $n > 117$ flies per genotype) Genotypes: *UAS-36(GGGGCC)/+; elavGS* ($n = 117$ flies), *UAS-36(GGGGCC); RpS25RNAi{GD10582}/elavGS/+* ($n = 120$ flies). **(h)** Expression of Rps25 RNAi line 2 alone in adult neurons (+RU) modestly extends lifespan of females flies relative to the un-induced control (-RU) (* $p = 0.0371$ by chi-squared log-rank test; $n = 131$ uninduced and $n = 131$ RNAi induced flies). Genotypes: *UAS-RpS25RNAi{GD10582}/elavGS*.

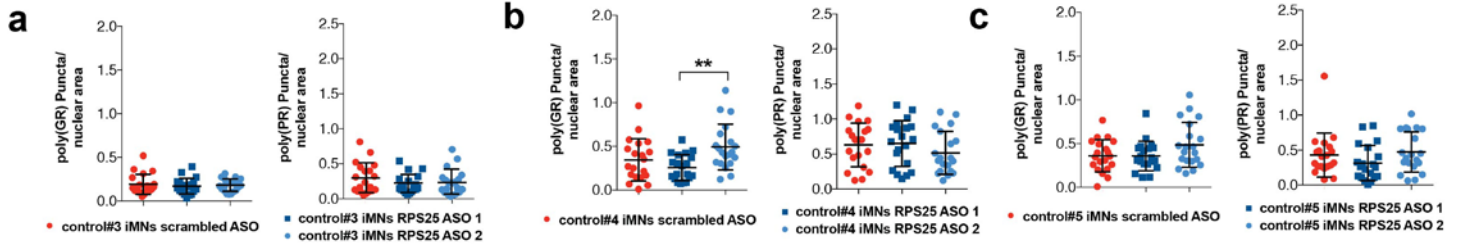


Supplementary Figure 8

Figure S8: RPS25-targeting ASOs reduce RPS25 expression and DPRs in c9ALS iMNs.

(a) RT-qPCR of *RPS25* RNA normalized by *ActB* RNA from iMNs treated for 72 hours with non-targeting or RPS25-targeting ASOs. There is a significant reduction in *RPS25* RNA in iMNs treated with RPS25-targeting ASOs (Two-way ANOVA with Tukey's multiple comparison; $n=3$ cell culture experiments; **** $p<0.0001$; mean \pm s.e.m.). (b) Quantification as in Fig. 3e of surviving induced motor neurons (iMNs) derived from 3 control iPSC lines treated with RPS25-targeting antisense oligonucleotides (ASO1 and 2) or control ASO control (two-sided log-rank tests; $n=3$ cell culture experiments, 50 iMNs per well were tracked and averaged per n ; ** $p=0.0069$, n.s., not significant $p=0.8147$; statistics from left to right: control iMNs control ASO vs. RPS25 ASO2, control ASO vs. RPS25 ASO1; mean \pm s.e.m.). (c) Survival plots for iMNs derived from a c9ALS iPSC line #4 and 3 control iPSC lines treated with RPS25-targeting antisense oligonucleotides (ASO1 and 2) or control ASO control (two-sided log-rank tests; $n=3$ cell culture experiments, 50 iMNs per well were tracked and averaged per n ; statistics from left to right: c9ALS#4 control ASO vs. control (**** $p<0.0001$), c9ALS #4 ASO1 vs. control ASO (* $p=0.0372$), c9ALS #4 ASO2 vs. control ASO (** $p=0.0237$). (d) Quantification of poly(GR) puncta normalized by nuclear area of c9ALS#4 iMNs in (one-way ANOVA, $n=20$ iMNs; ** $p=0.0019$, **** $p<0.0001$, mean \pm S.D.). (e) Quantification of poly(PR) puncta normalized by nuclear area of c9ALS #4 iMNs in (a) (one-way ANOVA, $n=20$ iMNs; **** $p<0.0001$; mean \pm S.D.). (f) Survival plots for iMNs derived from c9ALS iPSC line #5 (two-sided log-rank tests; $n=3$ cell culture experiments, 50 iMNs per well were tracked and averaged per n ; statistics from left to right: c9ALS #5 control ASO vs. control (**** $p<0.0001$), c9ALS #5 ASO1 vs. control ASO (** $p=0.0159$), c9ALS #5 ASO2 vs. control ASO (** $p=0.0231$). (g) Quantification of poly(GR) puncta normalized by nuclear area of c9ALS #5 iMNs (one-way ANOVA, $n=20$ iMNs; ** $p=0.0003$ (ASO1) and *** $p=0.0002$ (ASO2); mean \pm S.D.). (h) Quantification of

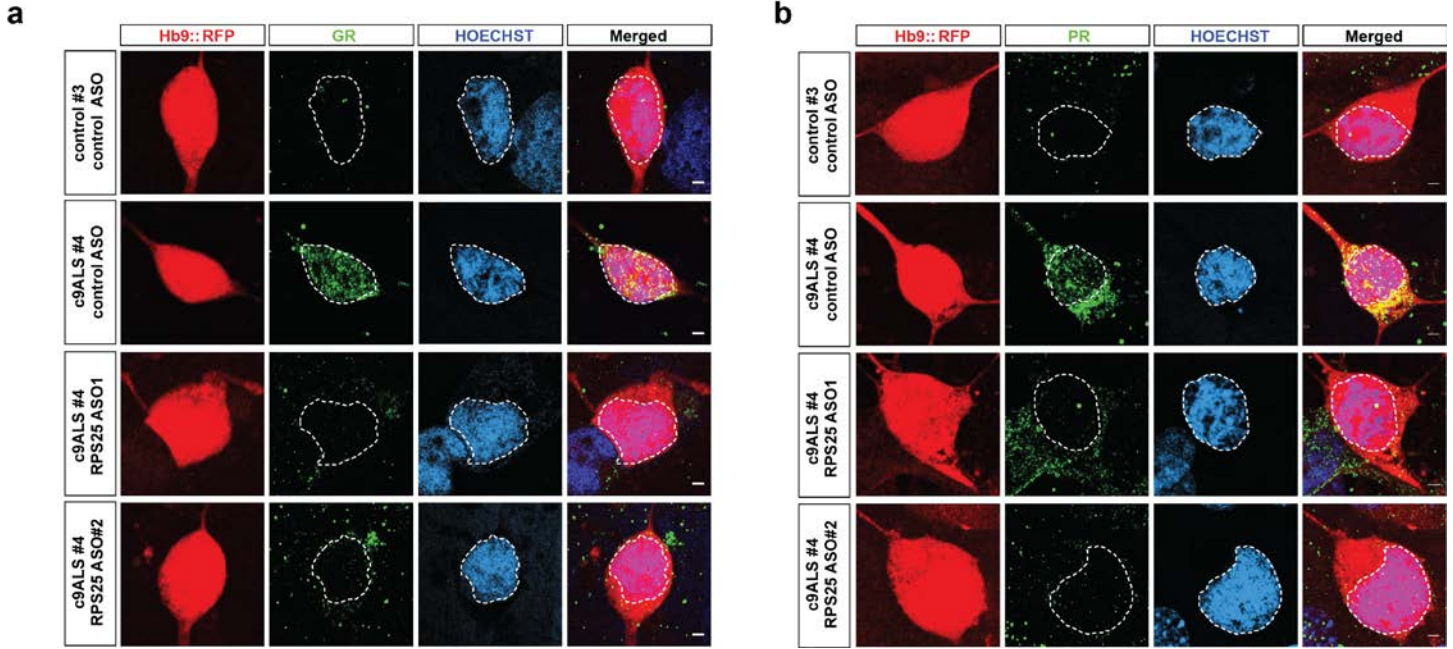
poly(PR) puncta normalized by nuclear area of c9ALS #5 iMNs (one-way ANOVA, n=20 iMNs; ****p<0.0001; mean +/-S.D.). (i) Survival plots for iMNs derived from c9ALS iPSC line #6 (two-sided log-rank tests; n=3 cell culture experiments, 20 iMNs per well were tracked and averaged per n; statistics from left to right: c9ALS #6 control ASO vs. control (****p<0.0001), c9ALS #6 ASO1 vs. control ASO (*p=0.0474), c9ALS #6 ASO2 vs. control ASO (*p=0.0354). (j) Quantification of poly(GR) puncta normalized by nuclear area of c9ALS #6 iMNs (one-way ANOVA, n=20 iMNs; (ASO1) *p=0.0186, (ASO2) *p=0.0482; mean +/-S.D.). (k) Quantification of poly(PR) puncta normalized by nuclear area of c9ALS #6 iMNs (one-way ANOVA, n=20 iMNs; (ASO1) ****p<0.0001, (ASO2) ***p=0.0002; mean +/-S.D.).



Supplementary Figure 9

Figure S9: RPS25-targeting ASOs on control iMNs.

(a) Quantification of poly(GR) (left) and poly(PR) (right) puncta normalized by nuclear area of control #3 iMNs in (one-way ANOVA with Tukey's multiple comparison test, $n=20$ iMNs; For GR: no significance (control vs ASO1) $p=0.7668$, (control vs ASO2) $p=0.9484$; For PR: no significance (control vs ASO1) $p=0.3388$, (control vs ASO2) $p=0.5754$; mean \pm S.D.). (b) Quantification of poly(GR) (left) and poly(PR) (right) puncta normalized by nuclear area of control #4 iMNs in (one-way ANOVA with Tukey's multiple comparison test, $n=20$ iMNs; For GR: no significance between other groups (control vs ASO1) $p=0.4294$, (control vs ASO2) $p=0.098$, (ASO1 vs ASO2) $**p=0.004$, For PR: no significance, (control vs ASO1) $p=0.9755$, (control vs ASO2) $p=0.4981$; mean \pm S.D.). (c) Quantification of poly(GR) (left) and poly(PR) (right) puncta normalized by nuclear area of control #5 iMNs in (one-way ANOVA with Tukey's multiple comparison test, $n=20$ iMNs; For GR: no significance between groups (control vs ASO1) $p=0.9992$, (control vs ASO2) $p=0.1395$, For PR: no significance between groups (control vs ASO1) $p=0.4089$, (control vs ASO2) $p=0.8765$; mean \pm S.D.).

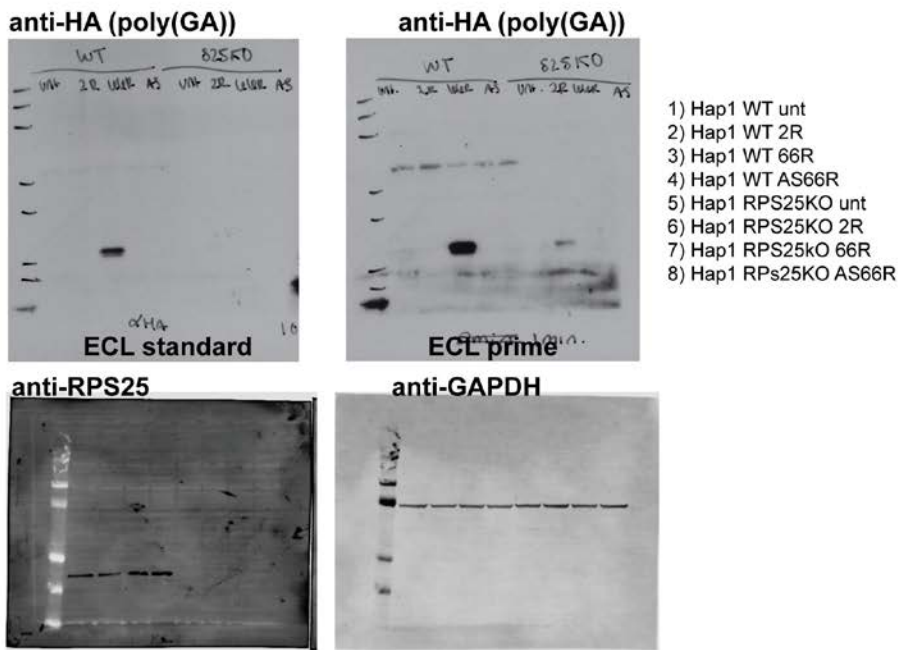


Supplementary Figure 10

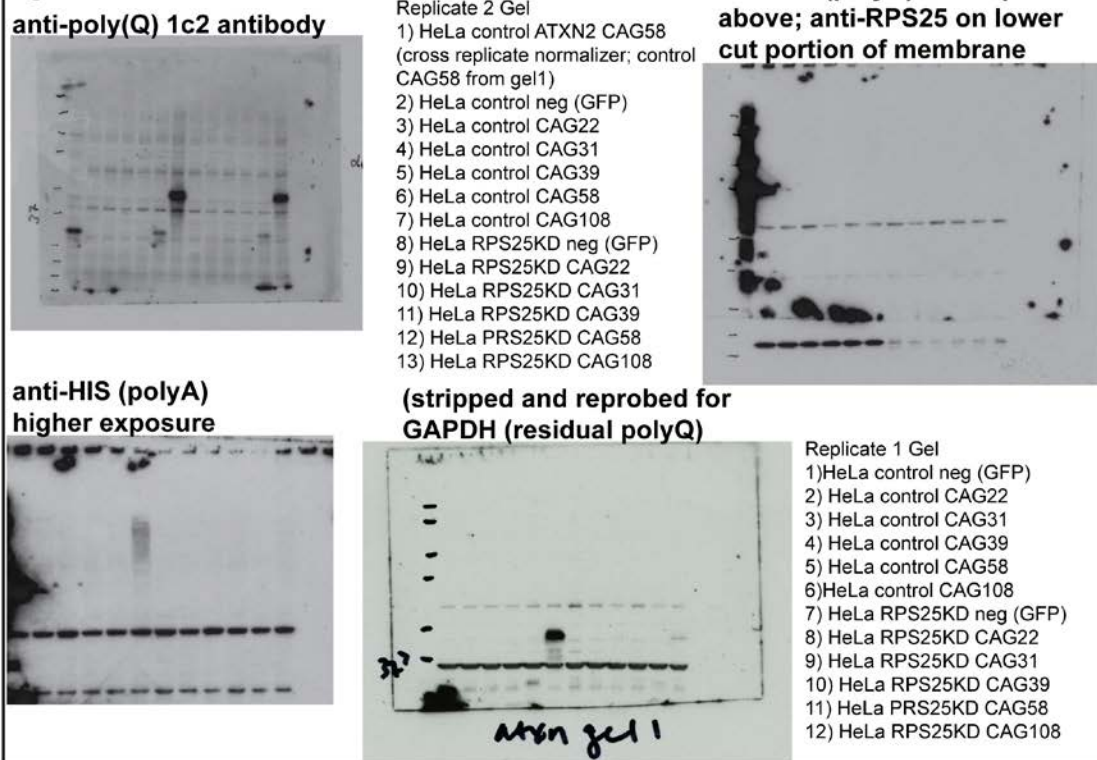
Figure S10: RPS25-targeting ASOs reduce nuclear DPR puncta in c9ALS iMNs.

(a) Representative immunocytochemistry images of poly(GR) puncta in control and patient-derived iMNs treated with control or RPS25-targeting ASOs quantified in Fig. 3f and Fig. S8. The number of poly(GR) puncta are counted per nuclear area in HB9-RFP+ iMNs. Dashed outline indicates nuclear region and scale bar is 2 μ m. Experiment was performed twice. (b) Representative immunocytochemistry images for poly(PR) puncta in control and patient-derived iMNs treated with control or RPS25-targeting ASOs quantified in Fig. 3g and Fig. S8. The number of poly(PR) puncta are counted per nuclear area in HB9-RFP+ iMNs. Dashed outline indicates nuclear region and scale bar is 2 μ m. Experiments were performed twice.

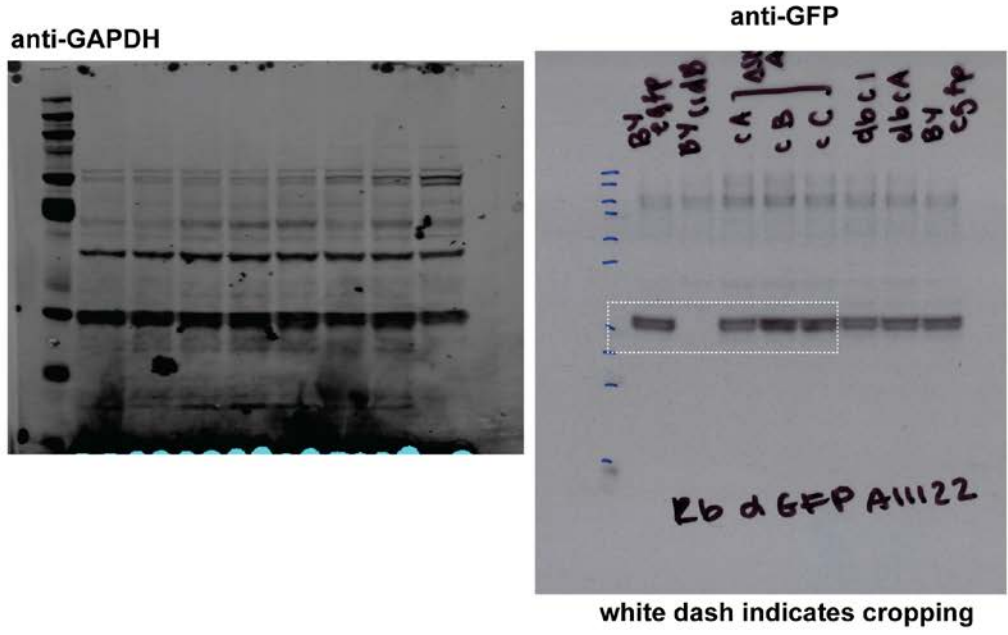
a Figure 1f: Hap1 C9 Blots



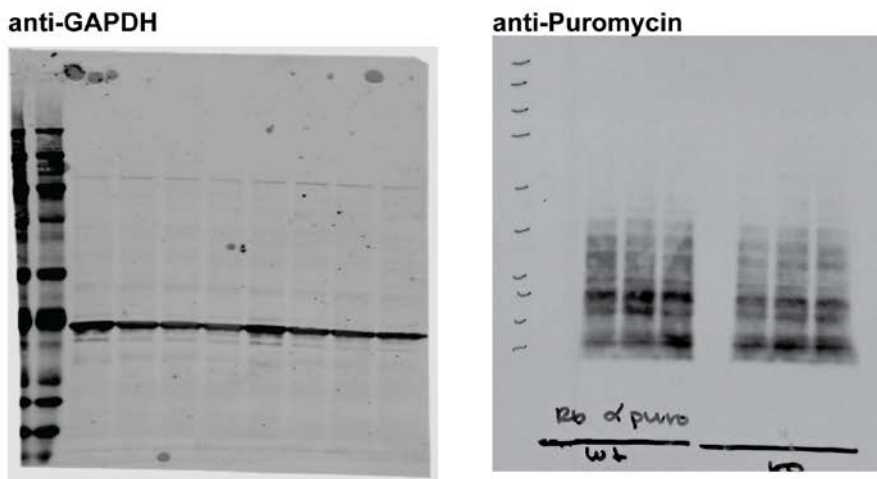
b Figure 1i: HeLa ATXN2 Blots

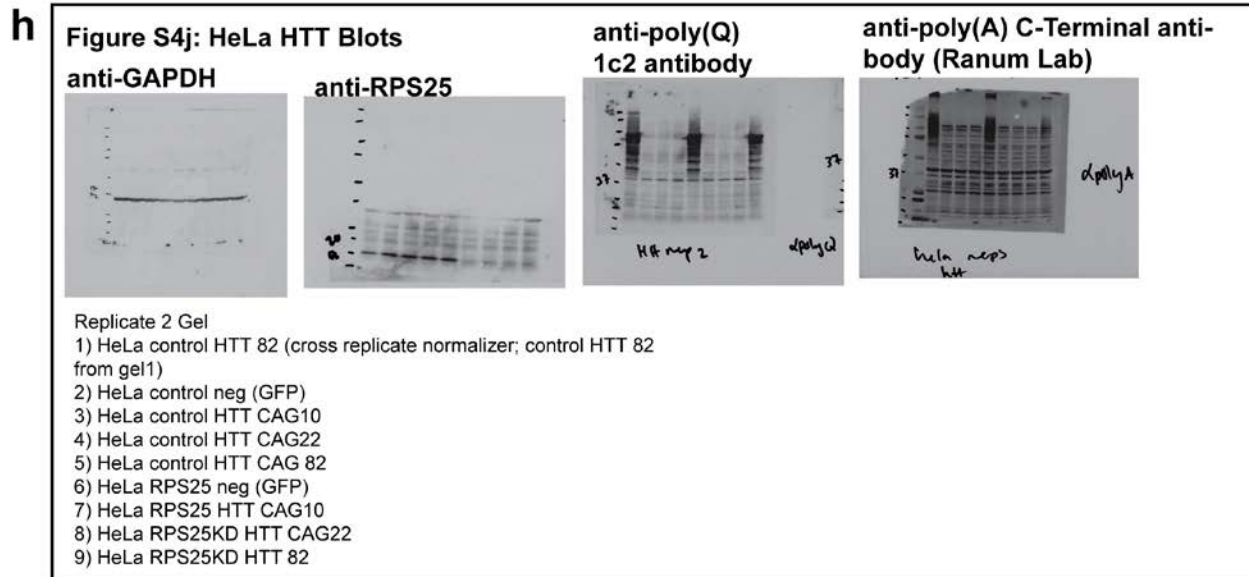
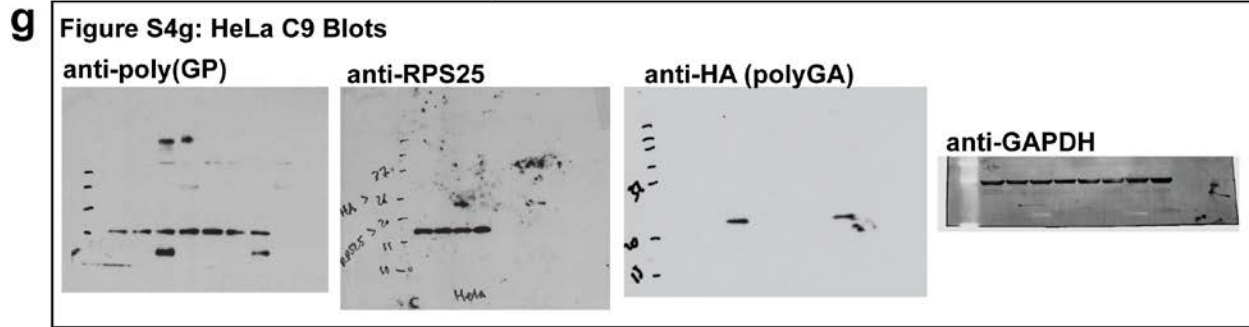
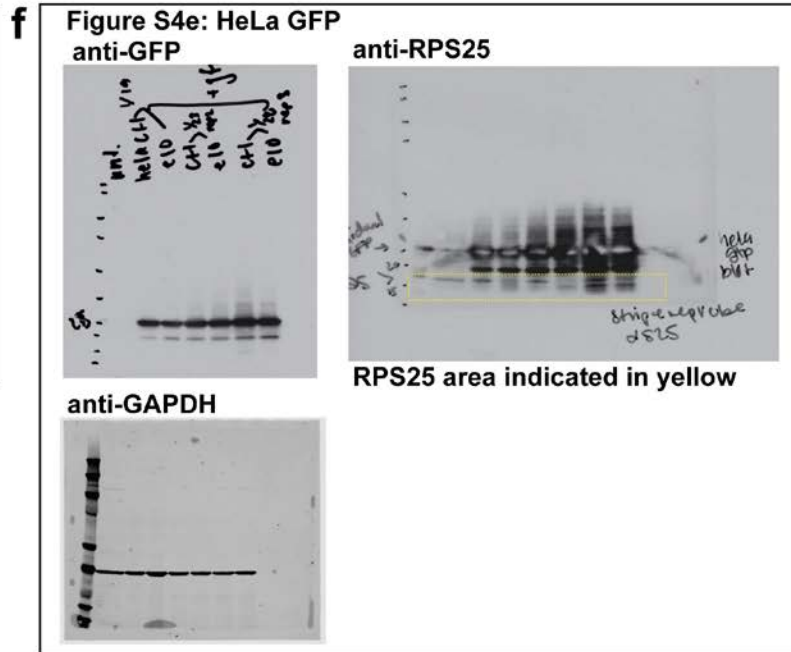
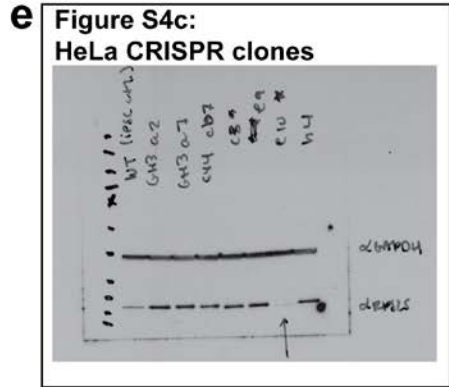


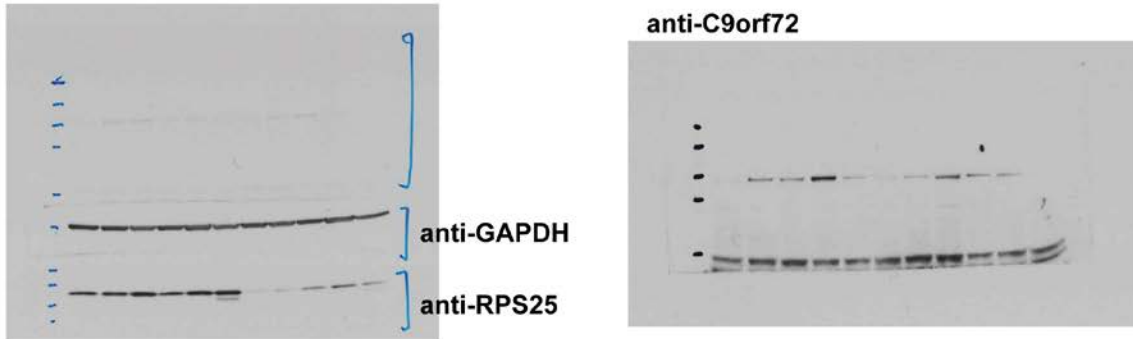
c Figure S1e: Yeast GFP



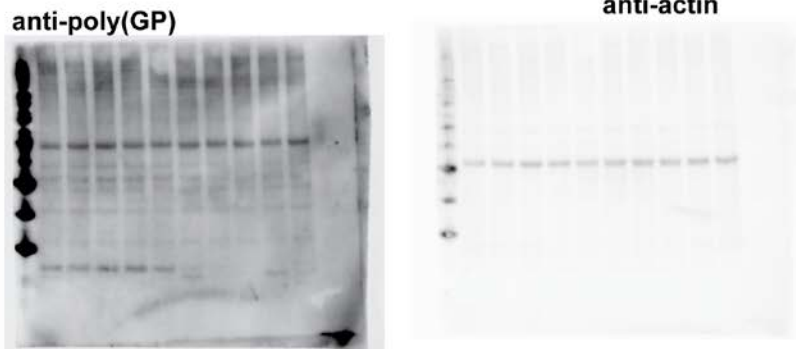
d Figure S2c: Hap1 Sunset/Puromycin incorporation





i**Fig. 2a and Fig. S5c: C9 iPSC blot w/ C9**

- | | |
|-------------------------------------|---------------------|
| 1) ipsc 33 unt (cross blot control) | 7) 2242 RPs25 siRNA |
| 2) 2242 NT siRNA | 8) 8783 RPS25 siRNA |
| 3) 8783 NT siRNA | 9) 33 RPS25 siRNA |
| 4) 33 NT siRNA | 10) 92 RPS25 siRNA |
| 5) 92 NT siRNA | 11) 002 RPS25 siRNA |
| 6) 002 NT siRNA | |

j**Fig. 3a: Drosophila poly(GP)****k****Fig. S7: Drosophila poly(GP)**

Supplementary Figure 11

Figure S11: Uncropped western blots from all figures and supplemental figures

(a-i) Precision Plus Kaleidoscope Standard (Bio Rad) for molecular weight markers was used and indicated on each blot. (j-k) MagicMark XP Western Protein Standard (Thermoscientific) for molecular weight markers was used and indicated on each blot.